

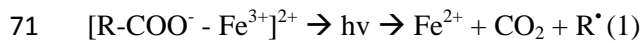
35 1. INTRODUCTION

36

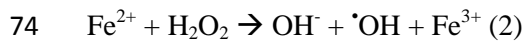
37 Advanced Oxidation Processes (AOPs) have been in the spotlight for more than three decades, as part
38 of a global effort to modernize actual methods of water disinfection. Their action is based on the
39 production of the extremely oxidizing hydroxyl radical ($\cdot\text{OH}$) [1], which can attack the chemical
40 structure of the microorganisms' cell wall and inactivate them [2]. Ultrasound has been extensively
41 studied as an AOP, targeting microorganism inactivation, such as bacteria, viruses etc., by either low
42 (~ 20 kHz) or high frequencies (200+ kHz) [2, 3, 4 and 5]. This method is exploiting the direct
43 mechanical action of the cavitation bubble implosion (low frequencies) as well as the additional
44 production of H_2O_2 and $\cdot\text{OH}$ radicals during cavitation (high frequencies); the propagation of
45 ultrasound waves in the aqueous medium initiates the aforementioned actions, by the generation of
46 extreme temperature and pressure conditions [6], which have a proven bactericidal effect [7, 8, 9, and
47 10].

48 As far as the ultrasound set-up is concerned, the frequency of the ultrasonic waves is a crucial
49 parameter, for it defines the size of the cavitation bubbles [11]. Literature suggests that the average
50 cavity size is proportional to the acoustic power and inversely proportional to the ultrasound frequency
51 [12]. It is also verified that apart from low frequency/high power ultrasound systems [13, 14], high
52 frequency/low power processes have been proven to efficiently inactivate microorganisms [8, 15, and
53 16]. However, ultrasound already requires high intensities to achieve total inactivation of
54 microorganisms, and therefore, is considered an expensive application for large volumes of water [2].
55 Considering all the above, it should be used preferably as a complementary disinfecting method [2].

56 The photo-Fenton process [17] could play the role of the main disinfecting method, as one of the most
57 efficient methods of hydroxyl radical production [18]. Lately, it has even been used to disinfect
58 drinking water, being a good alternative to chlorination, with its known disinfection by-products
59 formation [19]. However, wastewater is a complex matrix in which many organic and inorganic
60 compounds coexist, such as nutrients, salts and many substances that could influence the outcome of
61 the application of either process. It has been reported that the presence of hydroxyl radical scavengers,
62 namely the organic matter, presents an additional oxidation target and renders AOPs sensitive to the
63 treatment of wastewater [20, 21]. Suppression of these scavengers revealed their importance [10] and
64 also, for years the Fenton reaction was believed to be a pH-restricted reaction in highly acidic regions;
65 it was considered impossible to apply such methods, in matrices with near-neutral pH [22]. However,
66 recent advances [18, 23 and 24] have proven its effectiveness in the neutral area, and in the
67 simultaneous presence of organic matter [18, 25]. Previous work in our group has shown, there is no
68 need for acidification prior to the treatment to keep a significant part of the iron soluble; apart from the
69 direct complexation with bacteria, there are some strong photoactive Fe^{3+} complexes formed in presence
70 of organic matter [21, 25]:



72 The cycle continues with the reaction of the regenerated iron with hydrogen peroxide to produce more
73 hydroxyl radicals etc.



75 In order to increase the amount of water treated by solar-assisted methods, compound parabolic
76 collector reactors have been used [17, 18, 23 and 26], and solar photo-Fenton even was a subject under
77 question, because of the intermittent action of the light [27]. There is a technical issue to be addressed
78 in the intermittent nature of this treatment method, and the existence of “dead” time among the
79 experiment. Typically, a CPC photo-reactor consists of the illuminated surface and the storage-
80 recirculation tank. The recirculating flow of these reactors creates a gap in the illumination for as long
81 as water is present in the (dark) storage tank, allowing bacterial defense mechanisms to deploy [28].
82 Literature indicates a variety of light-to-dark distributions (Table 1), which materialize this difference
83 [17, 18, 23, 26, 29, 30 and 31].

84 Therefore, keeping in mind the improvement of the near-neutral photo-Fenton disinfection while
85 working within realistic operational parameters, for the first time we study the joint ultrasound/photo-
86 Fenton treatment for wastewater, in a CPC-like, lab-scale system. In this manner, we will take
87 advantage of two factors that could work complementing each other: firstly, the exploitation of the
88 dark intervals for sonication, along with the utilization of solar energy for the promotion of a mild
89 photo-Fenton reaction and secondly, the supplementary action these processes have, since, for
90 instance, US can produce H_2O_2 and subsequently, could fuel the photo-Fenton process. In our study,
91 synthetic secondary effluent was used, spiked with *E. coli* K12, recirculating around a sonicated dark
92 reactor and an illuminated batch reactor, under solar simulated light. We aim to:

- 93 i) Explore the effects of the photo-Fenton factors (light, reactants) and the ultrasonic action
94 (US) on both short and long-term disinfection events; clarification of the effects is
95 attempted by stepwise insertion of the participating actions.
- 96 ii) Investigate the involved operational parameters (recirculation speed, temperature, light
97 intensity, treated volume and distribution of volumes, iron and hydrogen peroxide content,
98 ultrasound intensity) in a small-scale set-up.

99

100 2. MATERIALS AND METHODS

101

102 2.1. Synthetic secondary effluent preparation

103

104 2.1.1. Microbial methods

105 The *E. coli* strain K12 (MG1655) employed was provided by the “Deutsche Sammlung von
106 Mikroorganismen und Zellkulturen”. Luria-Bertani broth was inoculated with a colony from bacterial
107 *E. coli* pre-cultures, placed in 50 ml plastic falcons for 8 h and then loop inoculated, after 1% dilution
108 overnight (180 rpm and 37°C for 15 h), to achieve stationary phase cells.

109 Harvested cells were centrifuged and washed three times (5000 rpm, 15 and 5 min for separation and
110 washing, respectively), followed by reservation in saline solution (neutral pH solution with 8 g/L NaCl
111 and 0.8 g/L KCl); a solution of 10^9 CFU/mL is achieved.

112

113 2.1.2. Synthetic wastewater composition

114 The preparation of the synthetic wastewater took place as under the directive of SYMAWE [32]. The
115 initial DOC was 100 mg/L (250 mg/L COD). The experiments used a 10% dilution (in distilled water)
116 of the said composition. The dilution performed corresponds to the COD and DOC values encountered
117 in normal secondary effluents. Finally, the pH of the sample was between 6.5-7. 1 mL of the prepared
118 bacterial solution was used to spike the diluted wastewater, thus resulting in an initial bacterial
119 population of 10^6 CFU/mL.

120

121 2.2. Reagents and analyses

122

123 The wastewater constituents, as well as the Fenton reagents were used as received. Photo-Fenton
124 experiments were carried out employing ferrous sulfate heptahydrate (Fluka Chemika), hydrogen
125 peroxide (35% by weight, Sigma Aldrich), used as received. The dissolved iron (Fe^{2+} , Fe^{3+}) was
126 measured with the ferrozine method [33], using a UV-Vis Lambda 20 spectrophotometer, provided by
127 PerkinElmer, Schwerzenbach, Switzerland. For 1.6 mL of sample 0.2 of ferrozine solution (4.9 mM)
128 was added, followed by 0.2 mL of hydroxylamine hydrochloride solution 10% w/w. Acetate buffer
129 solution was added for a final 4.5-5 pH value. To determine the concentration of hydrogen peroxide in
130 the sample titanium oxysulfate solution was added, also measured with the same spectrophotometer.
131 The pH of each sample was measured with a pH-meter provided by Mettler Toledo (PH/Ion S220,
132 Seven Compact, Mettler Toledo).

133

134 2.3. Description of reactors' set-up

135

136 The preliminary study was carried out in plain Pyrex glass batch reactors of 65 mL total capacity. In
137 the set-up presented in Figure 1, the configuration permits the sequential treatment of the synthetic

138 wastewater; US/photo-Fenton treatment was taking place (or vice versa). The same configuration was
139 used in one of our previous works, (used in [29], similar to the set-up used by Mendez-Arriaga et al,
140 2009 [34]), synthetic wastewater from a cylindrical double-wall glass vessel (400 mL) was pumped by
141 a peristaltic pump through three glass reactors (diameter 3.8 cm, effective irradiation surface 214.8
142 cm²), connected in series, of total volume 230 mL. Temperature was regulated by water recirculating
143 around the reactor and connected to a thermostat. The third reactor effluent was recirculated to the
144 original vessel. Normally, water was inserted in the double-wall reactor and pumped into the irradiated
145 part. Therefore, 230 mL of water were always present under illumination, 70 mL in the distribution
146 system and the rest subjected to sonication.

147 The ultrasonic waves (275 kHz) were emitted from a piezoelectric 4-cm disc, fixed on a Pyrex glass
148 plate adjusted to the bottom of the double-walled reactor. The intensities applied in all experiments
149 were 10, 20 and 40 W. The electric power was the chosen method to calibrate the ultrasonic
150 equipment. The in-series reactors were irradiated by the Suntest apparatus. The Suntest CPS solar light
151 simulator bears a lamp that emits ~0.5% of the photons at wavelengths <300 nm, ~7% between 300
152 and 400 nm and the rest follow the solar spectrum. The global irradiance values used in this work were
153 800, 1000 and 1200 W/m², while the corresponding UV values were approximately 19.2, 24.7
154 and 30.2 W/m².

155

156 2.4. Experimental design

157

158 Two sets of experiments were performed. In a first set of 8 experiments, that we call step-wise
159 construction of the joint treatment process, the elements of the US/hv/Fe/H₂O₂ were gradually and
160 accumulatively applied to the wastewater, in order to determine the individual role of each factor and
161 to detect any synergy among them. Table 2 shows the conditions corresponding to each individual
162 treatment factor when applied. Table 3 summarizes the four subsets of experiments in the step-wise
163 design.

164 In a second set of experiments (improvement of the process efficiency), eight different variables were
165 individually modified at three levels, while keeping the other variables constant, in order to obtain
166 improved working levels for each variable. Table 4 displays the three values (levels) essayed for each
167 variable. In each experiment the remaining parameters were kept constant and set to the central value
168 shown in the table.

169

170 2.5. Bacterial enumeration and regrowth tests

171

172 The disinfection efficiency was measured by viable plate counts on Petri dishes containing PCA agar
173 (plastic, 9-cm diameter). The pour-plating method was used and dilutions were made to ensure
174 countable numbers on the plates, i.e. 20-100 colonies/plate. Experiments were performed twice and
175 plating took place in 2-3 consequent dilutions and in duplicates.

176 Regrowth of bacteria was estimated after the storage of the samples at ambient temperature for 24 and
177 48 h after the sampling time. Samples were kept in 1.5 mL plastic Eppendorf caps in the dark and the
178 population was measured to assess the post-irradiation events, after their removal from the
179 experimental set-up.

180

181 3. RESULTS AND DISCUSSION

182

183 3.1. Results of the step-wise construction of the joint treatment process

184

185 As far as a potential application of mild photo-Fenton assisted by high frequency/low power
186 ultrasound is concerned, moderate concentrations of reactants are suggested for the evolution of our
187 study, after an initial investigation (data not shown). At 1000 W/m² light intensity, an addition of 1
188 ppm iron and 10 ppm of H₂O₂ will be used, as marginal values of Fenton reagents and 20 W of US
189 power.

190

191 3.1.1. Disinfection efficiency

192

193 *i) Experiments: 1-2 (WW and WW/Fe/H₂O₂).*

194 Figure 2a presents the results of the first part of the experiments, where neither light nor US was
195 applied. Wastewater was recirculated around the non-illuminated, non-sonicated experimental set-up
196 and the corresponding graphs describe the changes when H₂O₂ and iron were added to the solution.
197 We notice the increase of the population, when no reactants were added, due to the existence of
198 nutrients and salts that favor bacterial growth in this water matrix [35]. H₂O₂ is a substance with
199 disinfecting action, while iron itself is not toxic for bacteria. The addition of both reactants causes the
200 initiation of the Fenton reaction, which has a slow, but existing disinfecting ability and within a
201 timeframe of 4 h, we observe a 24.4% reduction in the initial population.

202

203 *ii) Experiments: 3-4 (US and US/Fe/H₂O₂).*

204 Figure 2b demonstrates the effects sonication has on samples, alongside with the stepwise insertion of
205 the Fenton reagents. The sample recirculates around the ultrasound vessel and the non-illuminated
206 area, being subject to intermittent high-frequency, low intensity sonication. When ultrasound alone is
207 applied, there is a decrease in total bacterial numbers, approaching 27.9%. The concurrent addition of
208 both Fenton reactants (H_2O_2 and Fe^{2+}) in the sonicated sample causes an 82.1% reduction in the
209 bacterial population, compared to 27.9 % reduction for US treatment and 24.4% for Fenton treatment
210 alone. This indicates a synergy between sonication and the Fenton reagents; a synergy factor of 1.57 is
211 demonstrated by the disinfecting efficiency of the reactions.

212 During sonication, the breakage of the cavitation bubbles can lead to the formation of an almost point-
213 sized heat source [36, 37], with local temperatures approaching 2000 K and pressures of 200 atm.
214 These extreme conditions can cause lysis of water molecules and along with that, extra production of
215 hydroxyl radicals [8]. The presence of the afore-mentioned particles in real wastewater and the
216 bacteria (in our matrix) could also play another important role, since the collapse of the cavitation
217 bubbles near a particle in the medium could cause micro-jets, depending on the size of the particle [38]
218 and could also form “weak spots” in the body of the liquid; these are potential places to form a cavity
219 [39]. It has been also reported that the presence of some salts causes a baro-protective effect on the
220 cells [40] and samples with higher contents of soluble solids would require higher sonication times.
221 Apart from the physical damage, during the ultrasound treatment of the sample, there is ample
222 generation of reactive oxygen species ($\cdot\text{OH}$ radicals [41], singlet oxygen [42, 43]), as mentioned
223 before, which are known to stress bacteria and lead to cell death [25, 44].

224 Finally, the addition of peptone (present in the synthetic wastewater) and the generally, presence of
225 nitrogen compounds has been reported to delay the sonicated degradation of phenols [45]. However,
226 nitrogen, under the presence of ultrasound waves can form NO_x (nitrate and nitrite). Its reaction with
227 singlet oxygen (as produced before) [43] produces peroxyxynitrite ($\text{ONOO}\cdot$) [46]. Peroxyxynitrite is
228 included in the reactive nitrogen species and can cause significant injures to various structures of the
229 cell (free radical damage or attack against the respiratory chain) [46].

230 The synergistic action of US and Fenton processes can be attributed to the exploitation of the
231 recombined H_2O_2 (from $\cdot\text{OH}$), which is less oxidative than the hydroxyl radical itself, and with that, the
232 re-initiation of the Fenton reaction with new reactants. Also, the ultrasound process, according to
233 Kryszczuk [47], increases the transient breakage of the bonds among the molecular components of the
234 cell membrane, which increases the permeability of the cell in external substances [48]. Therefore, the
235 introduction of Fe^{2+} in the cell is easier and its presence inside the cell can produce hydroxyl radicals
236 very close to vital functions of the cell, as well as the DNA [25] due to the induced internal Fenton
237 process.

238

239 *iii) Experiments: 5-6 ($h\nu$ and $h\nu/\text{Fe}/\text{H}_2\text{O}_2$).*

240 The 3rd set of experiments is dedicated in the investigation of the impact of light in the sequential
241 process. In all experiments light is provided at 1000 W/m², but in total, intermittent irradiation is
242 provided to the system; there is an illuminated regime and a non-illuminated one, in the Suntest
243 apparatus and the (inactive) sonication vessel (and tubing). In one of our previous works [29], we
244 demonstrated the impact light intermittence has on bacterial disinfection and survival, while
245 continuous supply or very fast recirculation around illuminated and dark regimes favors disinfection,
246 with the same set-up. Therefore, photo-Fenton is promoted in non-intermittent regimes or, as in our
247 case, short dark interval periods.

248 As it can be seen from Figure 2c, light, even in non-continuous form, is very effective and results in
249 high inactivation rates. Its disinfecting action is dominating the removal process, until the Fenton
250 reagents are present, and solar-assisted photo-Fenton is induced. The action of photo-Fenton is taking
251 place within the Suntest and dark (normal) Fenton takes place during the rest of the time, in a 0.85:1
252 time distribution (46% photo-Fenton over 54% Fenton). After an initial delay, which is demonstrated
253 as a shoulder in the graph, reaction is more effective by the $h\nu/Fe/H_2O_2$ than the corresponding solar
254 treatment.

255 Spuhler et al. [25] have reviewed the mechanism of bacterial inactivation by the photo-Fenton reaction
256 in near-neutral water with organic components, and have suggested the possible sources of ROS
257 production and cellular photo-oxidative damage, as well as the damage done by the ROS themselves,
258 deriving from the photo-Fenton reaction. In our suggested treatment method, these mechanisms are
259 completely compatible, explaining the majority of the actions and other works on near-neutral photo-
260 Fenton mechanisms describe fully the mechanisms, so we will not further analyze their findings.

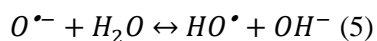
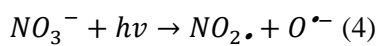
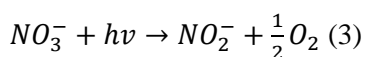
261

262 *iv) Experiments: 7-8 ($h\nu/US$ and $h\nu/US/Fe/H_2O_2$).*

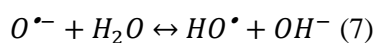
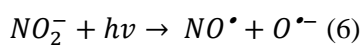
263 The final group of experiments are presented in Figure 2d. This graph summarizes the results of the
264 joint treatment by light and ultrasound. It is clear, after a comparison with Figure 2c, that when light is
265 present, its disinfecting action is dominating the process. However, we observe that the only case total
266 disinfection is achieved, is by the sequential US/pF system. In this system, wastewater spends its time
267 distributed 46% under photo-Fenton, 14% in the dark (dark-Fenton) and 40% in the sonication vessel
268 (US/Fenton). The experimental time has less inactive periods, and we observe that it has a significant
269 impact in the total inactivation of the bacterial populations in less than 4h. Here, the photo-Fenton/US
270 synergy is low in terms of bacterial counts, efficiency was improved in a relatively low percentage, but
271 only the coupled process resulted in total disinfection in 4 h. The elevated efficiency and total
272 inactivation for the first time, is attributed to the combination of all the previous actions (in US and/or
273 light), as well as the following actions (a graphical summary of all the actions is presented in Figure
274 3):

- 275 i. The hydroxyl radical is a short living ROS, and it occurs not to reach the target in all cases and
 276 often recombines to create H₂O₂ [49]. Therefore, the addition of ultrasound directly produces
 277 hydroxyl radicals and H₂O₂; the [•]OH directly attacks the cell and H₂O₂ participates in the
 278 photo-Fenton reaction (2). Alongside with the added H₂O₂, there is additional production,
 279 fueling the Fenton reaction and thus, improving the overall efficiency of the treatment.
- 280 ii. As we described before, with ultrasound waves, the loosening of transient bonds and insertion
 281 of Fe²⁺ in the cell is increased, which promotes the internal Fenton reaction. After the
 282 completion of the Fenton reaction, light reduces Fe³⁺ to Fe²⁺, and re-initiates a radical
 283 production inside the cell (internal photo-Fenton).
- 284 iii. Low frequency ultrasound has been proven [50] to reduce Fe³⁺ in the form of ferrous ions
 285 (Fe²⁺). The average size of the bubble however decreases when frequency is increased, in our
 286 system [12]; nevertheless, cavitation still takes place. Therefore, it is possible that an action
 287 like this could provide an additional source of iron available for the photo-Fenton process, and
 288 progress the regeneration of the catalyst in the (otherwise) non-illuminated part of the time. In
 289 that way, more available ferrous ions can be present in the solution.
- 290 iv. We mentioned the extreme temperature and pressure conditions that take place during the
 291 collapse of the cavitation bubbles. The interior part of the bubble, under these conditions, is
 292 known to emit light, under the phenomenon of sono-luminescence [8]. The optical aspects of
 293 this phenomenon have been studied [51] and the emitted light wavelengths fall into the
 294 necessary ones possibly able i) to induce the regeneration of the photo-Fenton reaction
 295 catalyst, ii) inflict direct UV damage to the cell. However, the necessary energy to achieve this
 296 is still under question.
- 297 v. Apart from the radicals' production through the normal photo-Fenton cycle, the presence of
 298 light is participating in another series of reactions with nitrogen compounds. The photolysis of
 299 nitrate and nitrites (produced by the participation of the US in the process) can lead to
 300 additional hydroxyl radical production [45]:

301 Photolysis of Nitrate:



305 Photolysis of Nitrite:



308

309 3.1.2. Post-processing events: long-term disinfecting activity of the joint process

310 The monitoring of the bacterial population for 48 h after the completion of the experiment has
311 indicated some rather interesting aspects on the characteristics of the driving forces of the joint
312 disinfection process. Figure 3e demonstrates the post-treatment bacterial counts, starting from the
313 moment the reactions have stopped (4-h mark). There are two big groups of charts we can distinguish,
314 which present different behavior: the non-irradiated and the irradiated processes.

315 First of all, it is observed that if there is no light or US treatment involved, as expected, bacterial
316 populations tend to increase their numbers. The presence of the Fenton reagents inflicts a constant, but
317 relatively slow, elimination of the present bacteria. The bacterial population in the sonicated samples
318 (square traces), although having survived the 4 hours of sonication, is significantly lowered in the days
319 following treatment. This observation seems to suggest some type of permanent damage that has
320 affected their cultivability. Even more, the US/Fenton treatment has shown that even with high
321 remaining bacterial values, after 2 days, the damaged bacteria have almost completely succumbed, due
322 to the combined sonication damage and the Fenton reaction that was still ongoing.

323 The long term effects caused by the sonication of the water sample can be summarized as follows: The
324 employed acoustic range promotes the production of hydrogen peroxide, which is an indicator of the
325 formation of other oxidative species [8]. In this frequency, the generated hydroxyl radicals are easily
326 transferred away from the bubbles [7, 52, 53 and 54]. The high-frequency damages include dislocation
327 of the cell membrane, which often leads to intracellular content leakage, due to the disruption of the
328 cell wall integrity [55, 56]. As a result, bacterial viability is lost; a gradual degradation of the cell
329 membrane takes place due to the attacks of the hydroxyl radicals in the medium and vital parts of the
330 bacterium are attacked [55], reduced potassium uptake and restricted DNA and protein synthesis have
331 also been reported [57]. Also, programmed cell death and cell apoptosis were also recently mentioned
332 [16, 58], which explain the delayed inactivation of cells. These processes can explain the behavior of
333 the sonicated samples for the 48-h monitoring period. Finally, in the combined process before, we
334 mentioned the greater iron uptake by the cells due to its transformation [47, 48]. We believe that this
335 process is of high significance, supported by the post irradiation events; within 48 h there are no more
336 cultivable bacteria, and comparing with the plain dark Fenton process, we attribute the change in the
337 already apoptotic cells, which are easier to succumb to further oxidative damage after their sonication
338 and finally to the increase of the internal Fenton process.

339 The second group of experiments, where light treatment was involved, all demonstrate zero counts
340 within two days. Light has significantly impaired bacterial reproduction and all samples that were
341 irradiated lead to total inactivation. Photo-Fenton treatment has proven to completely inactivate in less
342 time (<24 h), totally eradicating the small bacterial counts left during the treatment. Total inactivation
343 can however be reached within 24 h under joint US/solar light treatment even in the absence of iron,
344 due to the sequential damaging by US and solar light. No regrowth was observed in any of the

345 experiments within a 48h period. In addition to that, the coupled US/pF process, has maintained its
346 zero count throughout the 2-day period, with no noticeable regrowth or recovery.

347

348 3.2. Improvement of the process efficiency: Investigation of the operational parameters 349 involved in the US/pF coupling

350

351 Having observed the total and permanent inactivation for the solar-assisted US/pF system, it is our
352 interest to examine how other types of operational parameters could influence the process efficiency.
353 Possibilities for improving the process and investigating its flexibility and robustness are ample. The
354 parameters to be studied are summarized in Table 4, and divided in hydraulic, environmental and
355 chemical (US and Fenton factors).

356 3.2.1. Hydraulic parameters

357 Figures 4a-c present the investigation that has been conducted, to study the effects of the modification
358 of the recirculation rate, the number of in-series illuminated reactors, and the treated volume,
359 respectively. The three recirculation rates correspond to 1.87, 3.44 and 4.39 L/h. Hulsmans et al. [59]
360 suggest that increasing the flow rate in a US system resulted in higher disinfection rate. However, in
361 our system, changing the recirculation rate causes the faster sequential change from US to photo-
362 Fenton, and therefore, shorter cycles of treatment. This leads to more completed rounds of
363 sonication/Fenton, and consequently, better treatment results.

364 Figure 4a indicates the said effect; the explanation lies within the nature of the two actions. On the one
365 hand, sonication assists the inactivation and the transformation of iron more times, so photo-Fenton is
366 more efficient, and on the other hand, more completed cycles of illumination, provide higher
367 possibilities for the emitted photons to target the bacteria (direct action) or the production of hydroxyl
368 radicals to attack them (indirect action). Table 5 includes the hydraulic calculations concerning the
369 timeframe of the actions.

370 Furthermore, in Table 5 we notice the effect of changing the number of available reactors for the
371 photo-Fenton treatment. Reducing the number of reactors affects:

- 372 i) The available illuminated volume: The photo-Fenton action is also reduced, because less
373 volume is under illumination (reduction of both direct and indirect damage).
- 374 ii) The volume of the sonicated water: Since the volume remains 500 mL and the reactors of
375 ~75 mL are reduced, more water remains in the sonication chamber. Therefore, the ratio
376 of US power/volume of water is modified and less power (but more time) is available for
377 each mL of wastewater.

378 As a consequence, we observe in Figure 4b that reducing the available reactors from 3 to 1 modifies
379 the photo-Fenton to US treated volume ratio from 1.15 to 0.52 and 0.27, respectively (tubing volumes
380 are neglected, because of the slow rate of the dark Fenton reaction). In terms of bacterial numbers, the
381 inactivation rate is of 6, 4 and 3 $\log_{10}U$, for 3, 2 and 1 reactor available. Although this looks as a
382 diminishing effect on the process efficiency, it also indicates that if less irradiation is available, the
383 process is still effective, and an extension in the time would eventually lead to total inactivation. We
384 believe this is an indication of the assisting/complementary character of the sonication, whenever
385 photo-Fenton is not available.

386 Finally, although literature suggests that modifying the sonication volume has not a significant effect
387 on the efficiency of the sonication process (if the power-to volume ratio is respected) for bacterial
388 inactivation [59, 60], in Figure 4c we observe 2 and 3 $\log_{10}U$ of difference, respectively. A 20% and
389 40% increase of the volume lead to 33% and 50% reduction of the efficiency. This is explained by the
390 domination of the process by the photo-Fenton reaction, rather than the sonication; it seems that it is
391 not cost-effective to increase the total volume beyond a certain value.

392

393 3.2.2. Environmental influence

394 In our experimental set-up, an investigation of the temperature took place to assess the available
395 operating temperatures of the coupled treatment, summarized in Figures 5 a-b. The first operational
396 limit was the temperature of 30°C, to protect the piezoelectric disc. Recirculation of refrigerated water
397 around the mantle of the US vessel ensured that the temperature was maintained within this limit.
398 Reducing the operational temperature lead to decrease of the inactivation efficiency; the reaction
399 became slower and less effective. On the one hand, this behavior (Figure 5a) is attributed to the
400 reduced kinetics of the photo-Fenton reaction: it is known that temperature increases chemical
401 reactions' kinetics, plus Ortega-Gomez et al [61] revealed the reduced inactivation rate in another
402 bacterial species but also mesophilic with similar optimal growth temperature with *E. coli*, according
403 to the Arrhenius equation and on the other hand, treating wastewater at temperatures close to the
404 optimal growth conditions, can delay bacterial inactivation [62].

405 On the contrary, altering the irradiation intensity (Figure 5b) did not significantly affect the efficiency
406 of the process. It can be seen that $\pm 20\%$ difference in intensity resulted in similar required inactivation
407 times. The initial reaction kinetics is faster at 1200 W/m² because of the increased direct action of the
408 light; higher intensities lead to faster bacterial inactivation rates [63]. The process is nevertheless
409 effective even for lower intensities, suggesting that disinfection is possible even in days of low solar
410 radiation.

411

412 3.2.3. Fenton and sonication factors

413 Figures 6a-c present the results of the investigation over the constituents of the Fenton reaction, as
414 well as the only modifiable parameter of the US, the sonication power. We observe from figures 6a
415 and 6b, that there is a minimum quantity of the Fenton reagent required to be initially present, in order
416 to maintain the integrity of the reaction throughout the treatment time. For instance, when the initial
417 H_2O_2 concentration was reduced to 5 ppm, after the 2nd hour the reaction kinetics modified and
418 inactivation rate was impaired. The oxidation of organic matter by the hydroxyl radicals is competing
419 against the bacterial inactivation [21]. The contribution of photo-Fenton is reduced and the reaction
420 continues with the produced H_2O_2 and the direct effects of irradiation and US. However, doubling the
421 initial concentration of H_2O_2 , provides enough $\cdot\text{OH}$ radicals, to achieve the fastest inactivation time in
422 all our experiments. Although unique, this case suggests a doubling on the supply costs of the process,
423 but at the same time, a chance to improve otherwise impaired inactivation rates observed in previous
424 cases.

425 Same effects apply for the iron content of the initial sample. When the iron concentration was halved,
426 reaction rate and final outcome was mitigated, compared to the normal processes. Even though the US
427 indirect action benefits iron transformation to the more useful state of ferrous ions, as a catalyst, it is
428 obvious that it is in shortage. As soon as the initial concentration was doubled, no significant effect
429 was observed, probably due to the saturation of the sample although presence of organic matter
430 sustains iron in solution [21]. Hydroxyl radical production reached its peak and therefore no
431 improvement was observed in bacterial inactivation.

432 Finally, the modification of the acoustic power was investigated, and its effects on removal efficiency
433 are demonstrated in Figure 6c. Increasing US power results in higher particle breakage [64] and more
434 efficient removal, in the high frequencies [59, 60]. In our system, decreasing the power from 20 to 10
435 W, and consequently, the power-to-volume ratio, decreased the efficiency, although in a non-linear,
436 cost-effective manner; 50% reduction did not result to 50% decrease of the inactivation, but to 33%,
437 although the main target is total inactivation. This suggests that the process can operate in
438 economically low power, increasing its feasibility in real-scale application, and proves the
439 complementary character of the two processes. Increasing the power to 40 W did not really enhance
440 the removal efficiency, probably because 20 W was enough to induce the effects of sonication in the
441 sample or the increase was not high enough to demonstrate measurable change, in the hourly sample
442 scale.

443

444 3.3. Operational cost and full-scale application considerations

445

446 The proposed hybrid treatment has already been proven efficient against the treatment of pollutants in
447 bench scale [49] and the results found so far support its efficiency against *E. coli*. However, the

448 current set-up employs almost 40 kW/m³ electrical energy per hour, and compared with other low-
449 frequency sonication applications (e.g. [59] or [65]), the electrical energy required is much higher, in a
450 4-h scale. The sum drops if a higher amount is treated, but is still economically challenging. The main
451 problem is located in the drawback high frequency sonication engulfs, that requires long residence
452 times in order to achieve total disinfection, even with the aid of photo-Fenton. In order to render this
453 solution economically competitive some other factors need to be taken into account.

454 First of all, it was observed that high frequency disinfection did not dramatically increase disinfection
455 rates directly, but a long term inactivating effect was demonstrated. Sonicated samples after 48 h
456 presented lower bacterial counts, and null counts when the Fenton reagents were present. These results
457 indicate the possibility to reduce the residence times, and further investigate the correlation of
458 sonication with this long term inactivating effect. Hence, depending on the use of the treated water
459 afterwards, the residence time could differ, reducing the direct operational costs.

460 Furthermore, the investigation of the operational parameters, showed potential pathways to improve
461 the process. During this study, the contribution of each factor was studied separately. It was found that
462 e.g. doubling the base concentration of H₂O₂ (from 10 to 20 ppm) total inactivation was achieved in 3
463 h, almost 25% reduction in the residence time and increase of the iron concentration from 1 to 2 ppm
464 had no measurable effect, but the estimation of their combined effect is unknown. However, it is
465 normal to expect higher Fenton efficiency with higher reactant concentrations and further reduction of
466 the residence times, as well as improved rates with higher sonication power values. Therefore, a poly-
467 parametric design of experiments for the optimization of the system should be conducted, to define the
468 most economic operational conditions.

469 Concerning other photo-Fenton applications for pollutants degradation, Klammerth et al [66] used
470 values around 50 and 5 ppm for hydrogen peroxide and iron and Rodriguez-Chueca et al [67] used 5-
471 50 and 2.5-10 ppm, respectively. Switching from mild to normal photo-Fenton values for bacterial
472 inactivation in wastewater will holistically benefit the system efficiency. Apart from the direct photo-
473 Fenton effect which can be enhanced, a positive impact is also expected on the indirect effects of
474 sonication with the interactions with the iron content of the sample and the radical production. Finally,
475 a pilot scale plant, with optimized operational parameters could give a better view in the expected
476 operational costs. However, the marginal values used in this study indicated the promising potentials
477 of the system and suggested that the system has the possibility to be rendered economically feasible,
478 provided that long-term inactivation can be achieved by shorter sonication times.

479

480 4. CONCLUSIONS

481

482 An initial study concerning the treatment of wastewater microorganisms has been made, by the
483 application of sequential mode high frequency ultrasound and mild photo-Fenton. In the stepwise
484 introduction of treatment factors, light has been, by far, the most significant effect amongst all
485 parameters. Light alone has proven to be much more effective than US, Fenton, or the combination of
486 the two. Also, light combined with Fenton (photo-Fenton) and US with photo-Fenton (US-pF) have
487 been the two most effective disinfection options. This can be attributed to the well-known multi-level
488 effect of light, interpreted by the direct action of the light against bacteria, the indirect ROS production
489 and the direct role of light in Fe^{2+} reduction (photo-Fenton). High frequency-low intensity ultrasound
490 alone has not provided significant immediate bacterial reduction, but in long term, causes either
491 apoptotic behavior or increased susceptibility to the Fenton damage. When combined with light, US
492 has resulted in high inactivation rates in 4 h, and even higher when the Fenton reagents were also
493 introduced (joint US-pF process). This makes US-pF treatments an attractive alternative in permanent
494 (bacteriologically non-recurring) treatment methods.

495 Regarding the contribution of the operational parameters, temperature and volume introduce important
496 constraints: Temperature favors disinfection but must not exceed 30°C for US source protection;
497 increasing the sonication volume will result to higher US-to-pF ratios and lower efficiencies.
498 However, modification of the US-to-pF volume ratio can be opted regarding the post-treatment
499 handling of the sample; if immediate disinfecting action is required, pF can be promoted, in any other
500 case the continuous decay US causes will result to total inactivation during sample storage. Also,
501 addition of extra hydrogen peroxide and iron seemed to benefit bacterial inactivation. From the scope
502 of our work, the choice of mild photo-Fenton was satisfactory, but in a real application, this choice,
503 over normal amounts of reagents can be also altered depending on the requirements downstream.

504 Nevertheless, our results indicate that this US/pF process surpasses limitations that averted
505 installations of either one of the processes on wastewater treatment, such as the dead times in the dark
506 storage tanks, the power-to-volume ratio of the ultrasound, etc. It seems that the combination of the
507 two actions in sequential form helps overcome the disadvantages each method has separately;
508 whenever Fenton was limited, cellular regeneration was hindered by US, thus compensating during
509 dark periods and therefore improving photo-Fenton treatment efficiency. The two actions act
510 complementarily to each other, with ultrasound providing an additive effect in the photo-Fenton action
511 mode.

512

513 5. ACKNOWLEDGEMENTS

514

515 The authors wish to thank, in order of acquisition, the Mediterranean Office for Youth Program
516 (MOY, call 2011-2014), by means of which Stefanos Giannakis has received a PhD mobility grant
517 (MOY grant N°2010/044/01) in the joint Environmental Engineering Doctoral Program. Also, the

518 Swiss Government for the Swiss Government Excellence Scholarship, by means of which Stefanos
519 Giannakis has received a Research Visit fellowship (No. 2012.0499). Finally, Stefanos Papoutsakis
520 was funded by the Swiss-Hungarian Co-operation Program “Sustainable fine chemical,
521 pharmaceutical industry: screening and utilization of liquid wastes – Innovative approaches for the
522 abatement of industrial/toxic waste in aqueous effluents”.

523

524 6. REFERENCES

525

- 526 1. I. Oller, S. Malato, J.A. Sánchez-Pérez, W. Gernjak, M.I. Maldonado, L.A. Pérez-Estrada, C.
527 Pulgarín, A combined solar photocatalytic-biological field system for the mineralization of an
528 industrial pollutant at pilot scale, *Catalysis Today*, 122 (2007) 150-159.
- 529 2. A. Antoniadis, I. Poullos, E. Nikolakaki, D. Mantzavinos, Sonochemical disinfection of
530 municipal wastewater, *Journal of hazardous materials*, 146 (2007) 492-495.
- 531 3. P. Foladori, B. Laura, A. Gianni, Z. Giuliano, Effects of sonication on bacteria viability in
532 wastewater treatment plants evaluated by flow cytometry--fecal indicators, wastewater and activated
533 sludge, *Water research*, 41 (2007) 235-243.
- 534 4. C.V. Chrysikopoulos, I.D. Manariotis, V.I. Syngouna, Virus inactivation by high frequency
535 ultrasound in combination with visible light, *Colloids and surfaces. B, Biointerfaces*, 107 (2013) 174-
536 179.
- 537 5. T.J. Mason, E. Joyce, S.S. Phull, J.P. Lorimer, Potential uses of ultrasound in the biological
538 decontamination of water, *Ultrasonics sonochemistry*, 10 (2003) 319-323.
- 539 6. Y.T. Didenko, W.B. McNamara, K.S. Suslick, Hot spot conditions during cavitation in water,
540 *Journal of the American Chemical Society*, 121 (1999) 5817-5818..
- 541 7. I. Hua, M.R. Hoffmann, Optimization of ultrasonic irradiation as an advanced oxidation
542 technology, *Environmental Science & Technology*, 31 (1997) 2237-2243.
- 543 8. I. Hua, J.E. Thompson, Inactivation of *Escherichia coli* by sonication at discrete ultrasonic
544 frequencies, *Water research*, 34 (2000) 3888-3893.
- 545 9. M. Furuta, M. Yamaguchi, T. Tsukamoto, B. Yim, C. Stavarache, K. Hasiba, Y. Maeda,
546 Inactivation of *Escherichia coli* by ultrasonic irradiation, *Ultrasonics sonochemistry*, 11 (2004) 57-60.
- 547 10. M.F. Dadjour, C. Ogino, S. Matsumura, N. Shimizu, Kinetics of disinfection of *Escherichia*
548 *coli* by catalytic ultrasonic irradiation with TiO₂, *Biochemical Engineering Journal*, 25 (2005) 243-
549 248.
- 550 11. K.S. Suslick, *Sonochemistry*, *Science*, 247 (1990) 1439-1445.
- 551 12. A. Brotchie, F. Grieser, M. Ashokkumar, Effect of power and frequency on bubble-size
552 distributions in acoustic cavitation, *Physical review letters*, 102 (2009) 084302.
- 553 13. S. Drakopoulou, S. Terzakis, M. Fountoulakis, D. Mantzavinos, T. Manios, Ultrasound-
554 induced inactivation of gram-negative and gram-positive bacteria in secondary treated municipal
555 wastewater, *Ultrasonics sonochemistry*, 16 (2009) 629-634.
- 556 14. D. Venieri, E. Markogiannaki, E. Chatzisyneon, E. Diamadopoulos, D. Mantzavinos,
557 Inactivation of *Bacillus anthracis* in water by photocatalytic, photolytic and sonochemical treatment,
558 *Photochemical & Photobiological Sciences*, (2013).
- 559 15. R.V. Peterson, W.G. Pitt, The effect of frequency and power density on the ultrasonically-
560 enhanced killing of biofilm-sequestered *Escherichia coli*, *Colloids and Surfaces B: Biointerfaces*, 17
561 (2000) 219-227.

- 562 16. A. Moody, G. Marx, B.G. Swanson, D. Bermúdez-Aguirre, A comprehensive study on the
563 inactivation of *Escherichia coli* under nonthermal technologies: High hydrostatic pressure, pulsed
564 electric fields and ultrasound, *Food Control*, 37 (2014) 305-314.
- 565 17. A.-G. Rincón, C. Pulgarin, Fe³⁺ and TiO₂ solar-light-assisted inactivation of *E. coli* at field
566 scale: Implications in solar disinfection at low temperature of large quantities of water, *Catalysis*
567 *today*, 122 (2007) 128-136.
- 568 18. A. Moncayo-Lasso, J. Sanabria, C. Pulgarin, N. Benitez, Simultaneous *E. coli* inactivation and
569 NOM degradation in river water via photo-Fenton process at natural pH in solar CPC reactor. A new
570 way for enhancing solar disinfection of natural water, *Chemosphere*, 77 (2009) 296-300.
- 571 19. R.J. Bull, F.C. Kopfler, Health effects of disinfectants and disinfection by-products, AWWA,
572 1991.
- 573 20. T.M. Olson, P.F. Barbier, Oxidation kinetics of natural organic matter by sonolysis and ozone,
574 *Water research*, 28 (1994) 1383-1391.
- 575 21. E. Ortega-Gómez, M.M.B. Martín, B.E. García, J.A.S. Pérez, P.F. Ibáñez, Solar Photo-Fenton
576 for Water Disinfection: An Investigation of the Competitive Role of Model Organic Matter for
577 Oxidative Species, *Applied Catalysis B: Environmental*, (2013).
- 578 22. R.A. Torres, F. Abdelmalek, E. Combet, C. Petrier, C. Pulgarin, A comparative study of
579 ultrasonic cavitation and Fenton's reagent for bisphenol A degradation in deionised and natural waters,
580 *Journal of hazardous materials*, 146 (2007) 546-551.
- 581 23. F. Sciacca, J.A. Rengifo-Herrera, J. Wéthé, C. Pulgarin, Solar disinfection of wild *Salmonella*
582 sp. in natural water with a 18L CPC photoreactor: Detrimental effect of non-sterile storage of treated
583 water, *Solar Energy*, 85 (2011) 1399-1408.
- 584 24. J. Rodríguez-Chueca, M.I. Polo-López, R. Mosteo, M.P. Ormad, P. Fernández-Ibáñez,
585 Disinfection of real and simulated urban wastewater effluents using mild solar photo-Fenton, *Applied*
586 *Catalysis B: Environmental*.
- 587 25. D. Spuhler, J. Andrés Rengifo-Herrera, C. Pulgarin, The effect of Fe²⁺, Fe³⁺, H₂O₂ and the
588 photo-Fenton reagent at near neutral pH on the solar disinfection (SODIS) at low temperatures of
589 water containing *Escherichia coli* K12, *Applied Catalysis B: Environmental*, 96 (2010) 126-141.
- 590 26. P. Fernández, J. Blanco, C. Sichel, S. Malato, Water disinfection by solar photocatalysis using
591 compound parabolic collectors, *Catalysis Today*, 101 (2005) 345-352.
- 592 27. A.-G. Rincón, C. Pulgarin, Absence of *E. coli* regrowth after Fe³⁺ and TiO₂ solar
593 photoassisted disinfection of water in CPC solar photoreactor, *Catalysis today*, 124 (2007) 204-214.
- 594 28. D.B. Misstear, J.P. Murtagh, L.W. Gill, The Effect of Dark Periods on the UV Photolytic and
595 Photocatalytic Disinfection of *Escherichia coli* in a Continuous Flow Reactor, *Journal of Solar Energy*
596 *Engineering*, 135 (2013) 021012-021012.
- 597 29. S. Giannakis, A.I. Merino Gamo, E. Darakas, A. Escalas-Cañellas, C. Pulgarin, Impact of
598 different light intermittence regimes on bacteria during simulated solar treatment of secondary
599 effluent: Implications of the inserted dark periods, *Solar Energy*, 98, Part C (2013) 572-581.
- 600 30. J. Ndounla, S. Kenfack, J. Wéthé, C. Pulgarin, Relevant impact of irradiance (vs. dose) and
601 evolution of pH and mineral nitrogen compounds during natural water disinfection by photo-Fenton in
602 a solar CPC reactor, *Applied Catalysis B: Environmental*, 148-149 (2014) 144-153.
- 603 31. P. Fernández-Ibáñez, C. Sichel, M. Polo-López, M. de Cara-García, J. Tello, Photocatalytic
604 disinfection of natural well water contaminated by *Fusarium solani* using TiO₂ slurry in solar CPC
605 photo-reactors, *Catalysis Today*, 144 (2009) 62-68.
- 606 32. OECD Guidelines for Testing of Chemicals, Simulation Test-Aerobic Sewage Treatment
607 303A, 1999.
- 608 33. M. Gibbs, A simple method for the rapid determination of iron in natural waters, *Water*
609 *research*, 13 (1979) 295-297.

- 610 34. F. Mendez-Arriaga, R.A. Torres-Palma, C. Petrier, S. Esplugas, J. Gimenez, C. Pulgarin,
611 Ultrasonic treatment of water contaminated with ibuprofen, *Water research*, 42 (2008) 4243-4248.
- 612 35. J. Marugán, R. van Grieken, C. Pablos, C. Sordo, Analogies and differences between
613 photocatalytic oxidation of chemicals and photocatalytic inactivation of microorganisms, *Water*
614 *research*, 44 (2010) 789-796.
- 615 36. P. Butz, B. Tauscher, *Emerging technologies: chemical aspects*, *Food research international*,
616 35 (2002) 279-284.
- 617 37. P. Fellows, *Food processing technology: Principles and practice*. (2000) 2nd ed., CRC Press,
618 New York
- 619 38. E.R. Holm, D.M. Stamper, R.A. Brizzolara, L. Barnes, N. Deamer, J.M. Burkholder,
620 Sonication of bacteria, phytoplankton and zooplankton: Application to treatment of ballast water,
621 *Marine pollution bulletin*, 56 (2008) 1201-1208.
- 622 39. T. Leighton, *The acoustic bubble*, Access Online via Elsevier, 1994.
- 623 40. A. Molina-Höppner, W. Doster, R.F. Vogel, M.G. Gänzle, Protective effect of sucrose and
624 sodium chloride for *Lactococcus lactis* during sublethal and lethal high-pressure treatments, *Applied*
625 *and environmental microbiology*, 70 (2004) 2013-2020.
- 626 41. C. Petrier et al, in: T.J. Mason, A. Tiehm, *Advances in Sonochemistry*, Volume 6: Ultrasound
627 in Environmental Protection, Access Online via Elsevier, 2001
- 628 42. R.S. Davidson, A. Safdar, J.D. Spencer, B. Robinson, Applications of ultrasound to organic
629 chemistry, *Ultrasonics*, 25 (1987) 35-39.
- 630 43. Y. Matsumura, A. Iwasawa, T. Kobayashi, T. Kamachi, T. Ozawa, M. Kohno, Detection of
631 High-frequency Ultrasound-induced Singlet Oxygen by the ESR Spin-trapping Method, *Chemistry*
632 *Letters*, 42 (2013) 1291-1293.
- 633 44. J. Ndounla, D. Spuhler, S. Kenfack, J. Wéthé, C. Pulgarin, Inactivation by solar photo-Fenton
634 in pet bottles of wild enteric bacteria of natural well water: Absence of re-growth after one week of
635 subsequent storage, *Applied Catalysis B: Environmental*, 129 (2013) 309-317.
- 636 45. F. Zaviska, P. Drogui, E.M. El Hachemi, E. Naffrechoux, Effect of nitrate ions on the
637 efficiency of sonophotochemical phenol degradation, *Ultrasonics sonochemistry*, 21 (2014) 69-75.
- 638 46. E. Novo, M. Parola, Redox mechanisms in hepatic chronic wound healing and fibrogenesis,
639 *Fibrogenesis & tissue repair*, 1 (2008) 5.
- 640 47. M.D. Kryszczuk, *The effect of ultrasound in a chemotherapeutic study of ascites tumor cells*,
641 in, Catholic University of America Press, Washington, 1962.
- 642 48. E. Dahl, Physicochemical aspects of disinfection of water by means of ultrasound and ozone,
643 *Water research*, 10 (1976) 677-684.
- 644 49. R.A. Torres, G. Sarantakos, E. Combet, C. Pétrier, C. Pulgarin, Sequential helio-photo-Fenton
645 and sonication processes for the treatment of bisphenol A, *Journal of Photochemistry and*
646 *Photobiology A: Chemistry*, 199 (2008) 197-203.
- 647 50. M. Chauhan, Effect of ultrasound on the redox reactions of iron (II) and (III), *Indian journal of*
648 *chemistry. Sect. A: Inorganic, physical, theoretical & analytical*, 43 (2004) 2098-2101.
- 649 51. Y.T. Didenko, S. Pugach, Spectra of water sonoluminescence, *The Journal of Physical*
650 *Chemistry*, 98 (1994) 9742-9749.
- 651 52. C. Petrier, A. Jeunet, J.L. Luche, G. Reverdy, Unexpected frequency effects on the rate of
652 oxidative processes induced by ultrasound, *Journal of the American Chemical Society*, 114 (1992)
653 3148-3150.
- 654 53. C. Petrier, M.-F. Lamy, A. Francony, A. Benahcene, B. David, V. Renaudin, N. Gondrexon,
655 Sonochemical degradation of phenol in dilute aqueous solutions: comparison of the reaction rates at 20
656 and 487 kHz, *The Journal of Physical Chemistry*, 98 (1994) 10514-10520.
- 657 54. C. Petrier, B. David, S. Laguian, Ultrasonic degradation at 20 kHz and 500 kHz of atrazine
658 and pentachlorophenol in aqueous solution: Preliminary results, *Chemosphere*, 32 (1996) 1709-1718.

659 55. S. Koda, M. Miyamoto, M. Toma, T. Matsuoka, M. Maebayashi, Inactivation of *Escherichia*
660 *coli* and *Streptococcus mutans* by ultrasound at 500kHz, *Ultrasonics sonochemistry*, 16 (2009) 655-
661 659.

662 56. E. Joyce, A. Al-Hashimi, T. Mason, Assessing the effect of different ultrasonic frequencies on
663 bacterial viability using flow cytometry, *Journal of applied microbiology*, 110 (2011) 862-870.

664 57. C.N. Haas, R.S. Engelbrecht, Physiological alterations of vegetative microorganisms resulting
665 from chlorination, *Journal (Water Pollution Control Federation)*, (1980) 1976-1989.

666 58. S. Broekman, O. Pohlmann, E.S. Beardwood, E.C. de Meulenaer, Ultrasonic treatment for
667 microbiological control of water systems, *Ultrasonics sonochemistry*, 17 (2010) 1041-1048.

668 59. A. Hulsmans, K. Joris, N. Lambert, H. Rediers, P. Declerck, Y. Delaedt, F. Ollevier, S. Liers,
669 Evaluation of process parameters of ultrasonic treatment of bacterial suspensions in a pilot scale water
670 disinfection system, *Ultrasonics sonochemistry*, 17 (2010) 1004-1009.

671 60. A. Al Bsoul, J.P. Magnin, N. Commenges-Bernole, N. Gondrexon, J. Willison, C. Petrier,
672 Effectiveness of ultrasound for the destruction of *Mycobacterium* sp. strain (6PY1), *Ultrasonics*
673 *sonochemistry*, 17 (2010) 106-110.

674 61. E. Ortega-Gomez, P. Fernandez-Ibanez, M.M. Ballesteros Martin, M.I. Polo-Lopez, B.
675 Esteban Garcia, J.A. Sanchez Perez, Water disinfection using photo-Fenton: Effect of temperature on
676 *Enterococcus faecalis* survival, *Water research*, 46 (2012) 6154-6162.

677 62. S. Giannakis, E. Darakas, A. Escalas-Cañellas, C. Pulgarin, The antagonistic and synergistic
678 effects of temperature during solar disinfection of synthetic secondary effluent, *Journal of*
679 *Photochemistry and Photobiology A: Chemistry*, 280 (2014) 14-26.

680 63. A. Rincon, C. Pulgarin, Photocatalytical inactivation of *E. coli*: effect of (continuous–
681 intermittent) light intensity and of (suspended–fixed) TiO₂ concentration, *Applied Catalysis B:*
682 *Environmental*, 44 (2003) 263-284.

683 64. V. Raman, A. Abbas, Experimental investigations on ultrasound mediated particle breakage,
684 *Ultrasonics sonochemistry*, 15 (2008) 55-64.

685 65. E. Joyce, S.S. Phull, J.P. Lorimer, T.J. Mason, The development and evaluation of ultrasound
686 for the treatment of bacterial suspensions. A study of frequency, power and sonication time on
687 cultured *Bacillus* species, *Ultrasonics sonochemistry*, 10 (2003) 315-318.

688 66. N. Klamerth, S. Malato, A. Agüera, A. Fernández-Alba, G. Mailhot, Treatment of Municipal
689 Wastewater Treatment Plant Effluents with Modified Photo-Fenton As a Tertiary Treatment for the
690 Degradation of Micro Pollutants and Disinfection, *Environmental Science & Technology*, 46 (2012)
691 2885-2892.

692 67. J. Rodríguez-Chueca, M.I. Polo-López, R. Mosteo, M.P. Ormad, P. Fernández-Ibáñez,
693 Disinfection of real and simulated urban wastewater effluents using a mild solar photo-Fenton,
694 *Applied Catalysis B: Environmental*, 150–151 (2014) 619-629.

695

697 *Table 1 – Hydraulic characteristics of previous works in CPC reactors*

	Flow rate (L/min)	Total volume (L)	Volume-to- flowrate ratio	Illuminated Volume	Volume in the dark	Light-to- dark ratio
Fernandez- Ibañez et al. (2009)	20	14	0.70	32%	68%	0.47
Moncayo- Lasso et al. (2009)	17.5	20	1.14	45%	55%	0.82
Fernandez- Ibañez et al. (2005) (varied flowrates)	5, 13, 22.5	11	2.2, 0.85, 0.49	49%	51%	0.96
Rincon & Pulgarin (2007) (min, max capacity)	20.5	37, 70	1.80, 3.41	65%, 34%	35%, 66%	1.86, 0.52
Sciacca et al. (2011)	24.2	18	0.74	83%	17%	4.88
Giannakis et al. (2013)	0.03, 0.06, 0.07	0.7	22.58, 12.28, 9.59	33%	67%	0.49
Ndounla et al. (2013)	2	25	12.5	60%	40%	1.53

698

699 *Table 2 – Parameters involved in the joint treatment process*

Factors	Values	Other parameters
Light	1000 W/m ²	<i>Temperature: 30 °C</i>
Ultrasound	20 W	<i>Recirculating Flow rate: 4.39 L/h</i>
Iron	1 ppm	<i>Treated Volume: 500 mL</i>
H₂O₂	10 ppm	<i>Initial Population: 10⁶ CFU/mL</i>

700

701

702 **Table 3 – Subsets of experiments in the step-wise construction of the joint $h\nu/US/Fe/H_2O_2$**
 703 **treatment process.**

Experiments	Treatment constituents
1-2	WW and WW/Fe/H ₂ O ₂ - Wastewater with no treatment - Wastewater + Fe/H ₂ O ₂
3-4	US and US/Fe/H ₂ O ₂ - Wastewater+US - Wastewater+US+Fe/H ₂ O ₂
5-6	$h\nu$ and $h\nu/Fe/H_2O_2$ - Light - Light+/Fe/H ₂ O ₂ (photo-Fenton)
7-8	$h\nu/US$ and $h\nu/US/Fe/H_2O_2$ - Light+US - US+photo-Fenton

704

705 **Table 4 – Overview of the investigation of the operational parameters**

Factors¹	Level 1	Level 2	Level 3
Hydraulic			
<i>Pump rpm</i>	33	66	99
<i>No. of Illuminated vessels</i>	1	2	3
<i>Wastewater volume (mL)</i>	500	600	700
Environmental			
<i>Temperature (°C)</i>	10	20	30
<i>Light Intensity (W/m²)</i>	800	1000	1200
Fenton / Ultrasound			
<i>H₂O₂ Concentration (ppm)</i>	5	10	20
<i>Fe Concentration (ppm)</i>	0.5	1	2
<i>US Acoustic Power (W)</i>	10	20	40

706 ¹Central values are annotated with bold.

707

Increasing recirculation speed from 33 to 99 rpm (1.87 to 4.39 L/h)

Reactors	3	33	rpm	Reactors	3	66	rpm	Reactors	3	99	rpm
-----------------	----------	-----------	------------	-----------------	----------	-----------	------------	-----------------	----------	-----------	------------

Table 5 – Hydraulic calculations on the reactor set-up

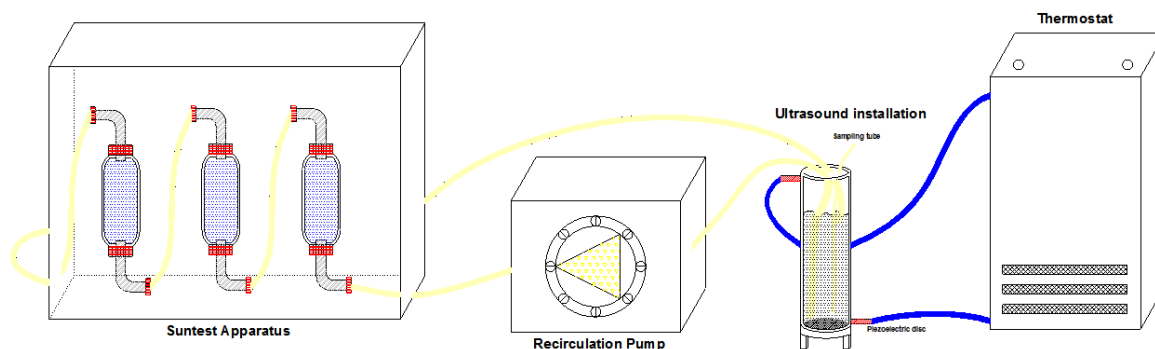
Volume	500	mL	1.87	L/h	1.87	L/h	Volume	500	mL	3.44	L/h	3.44	L/h	Volume	500	mL	4.39	L/h	4.39	L/h
Light	230	mL	7.38	min	46	%	Light	230	mL	4.01	min	46	%	Light	230	mL	3.14	min	46	%
Tubing	70	mL	2.25	min	14	%	Tubing	70	mL	1.22	min	14	%	Tubing	70	mL	0.96	min	14	%
US	200	mL	6.42	min	40	%	US	200	mL	3.49	min	40	%	US	200	mL	2.73	min	40	%
Total	500	mL	16.04	min	100	%	Total	500	mL	8.72	min	100	%	Total	500	mL	6.83	min	100	%

Increasing illuminated volume from 1 reactor to 3 (75 to 230 mL)

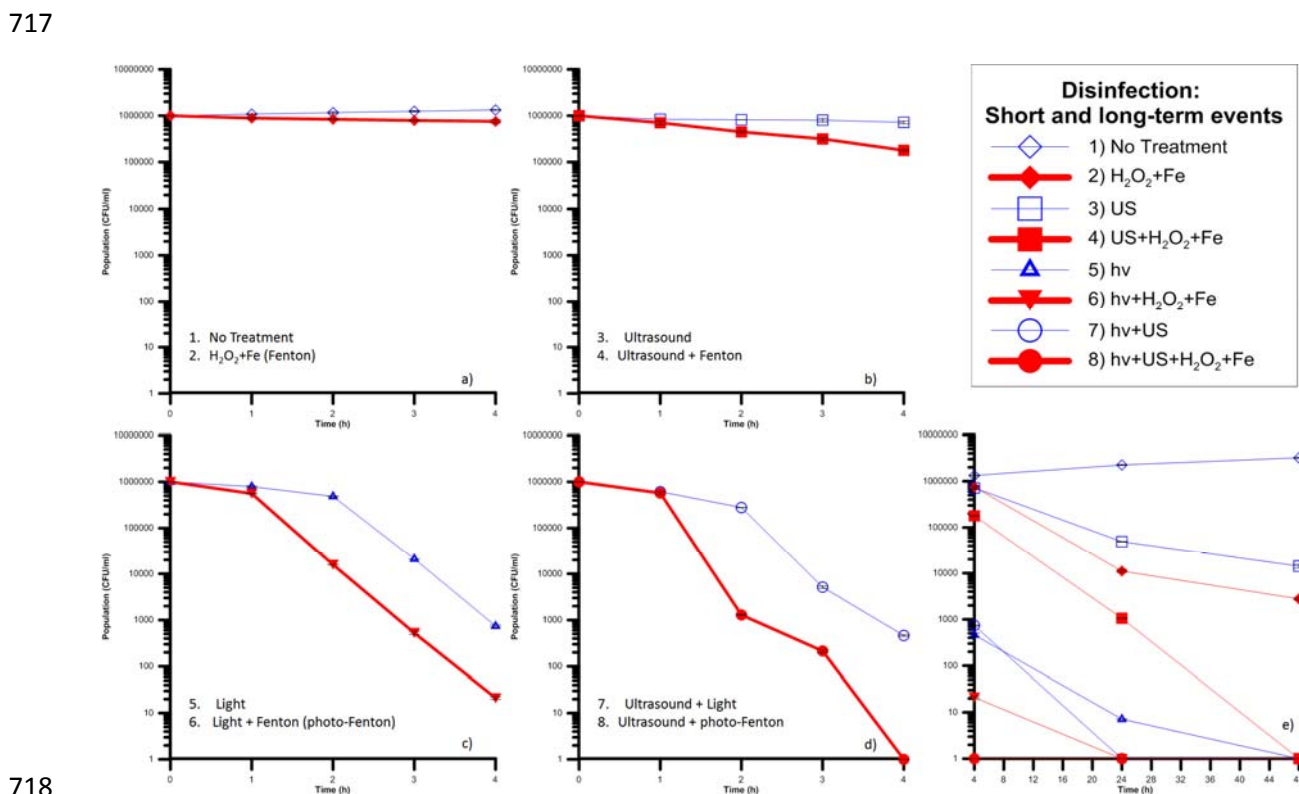
Reactors	1	99	rpm	Reactors	2	99	rpm	Reactors	3	99	rpm									
Volume	500	mL	4.39	L/h	4.39	L/h	Volume	500	mL	4.39	L/h	4.39	L/h	Volume	500	mL	4.39	L/h	4.39	L/h
Light	75	mL	1.03	min	15	%	Light	150	mL	2.05	min	30	%	Light	230	mL	3.14	min	46	%
Tubing	50	mL	0.68	min	10	%	Tubing	60	mL	0.82	min	12	%	Tubing	70	mL	0.96	min	14	%
US	375	mL	5.13	min	75	%	US	290	mL	3.96	min	58	%	US	200	mL	2.73	min	40	%
Total	500	mL	6.83	min	100	%	Total	500	mL	6.83	min	100	%	Total	500mL	mL	6.83	min	100	%

Increasing total treated volume from 500 to 700 mL

Reactors	3	99	rpm	Reactors	3	99	rpm	Reactors	3	99	rpm									
Volume	500	mL	4.39	L/h	4.39	L/h	Volume	600	mL	4.39	L/h	4.39	L/h	Volume	700	mL	4.39	L/h	4.39	L/h
Light	230	mL	3.14	min	46	%	Light	230	mL	3.14	min	38	%	Light	230	mL	3.14	min	33	%
Tubing	70	mL	0.96	min	14	%	Tubing	70	mL	0.96	min	12	%	Tubing	70	mL	0.96	min	10	%
US	200	mL	2.73	min	40	%	US	300	mL	4.10	min	50	%	US	400	mL	5.47	min	57	%
Total	500	mL	6.83	min	100	%	Total	600	mL	8.20	min	100	%	Total	700	mL	9.57	min	100	%

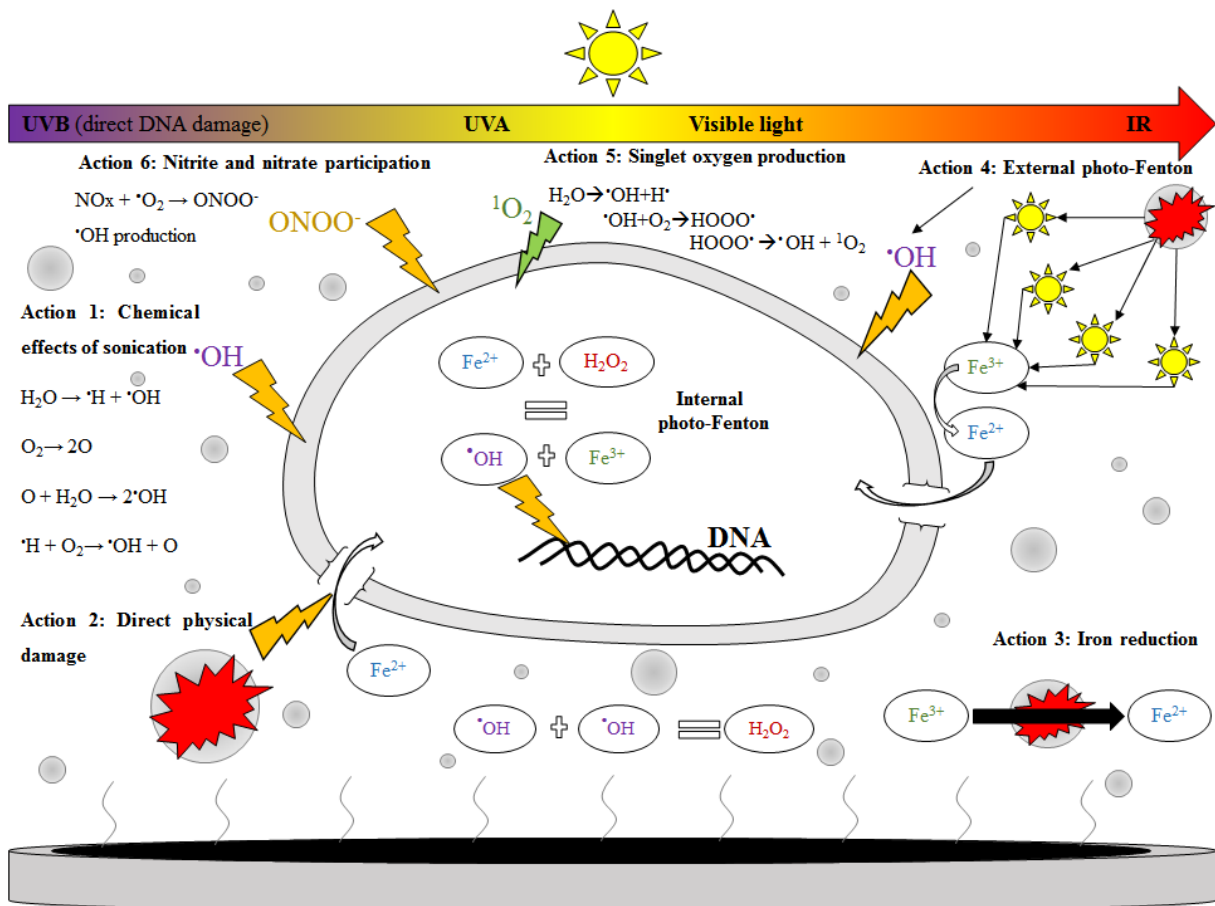


713
 714 Figure 1 – Experimental set-up, consisting of the illuminated area (Suntest apparatus), the recirculation pump,
 715 the (dark) sonication vessel and the temperature control (thermostat). The flow direction is clockwise, water is
 716 introduced at surface level and sampled from the bottom of the vessel.



718
 719 Figure 2 – Experimental results from the coupling of photo-Fenton and sonication. a) Experiments 1-2 (WW and
 720 WW/Fe/H₂O₂), b) Experiments 3-4 (US and US/Fe/H₂O₂), c) Experiments 5-6 ($h\nu$ and $h\nu/Fe/H_2O_2$) and d)
 721 Experiments 7-8 ($h\nu/US$ and $h\nu/US/Fe/H_2O_2$). e) Long-term inactivation events for 48 h (time axis initiates in the
 722 4-h mark, after treatment).

723



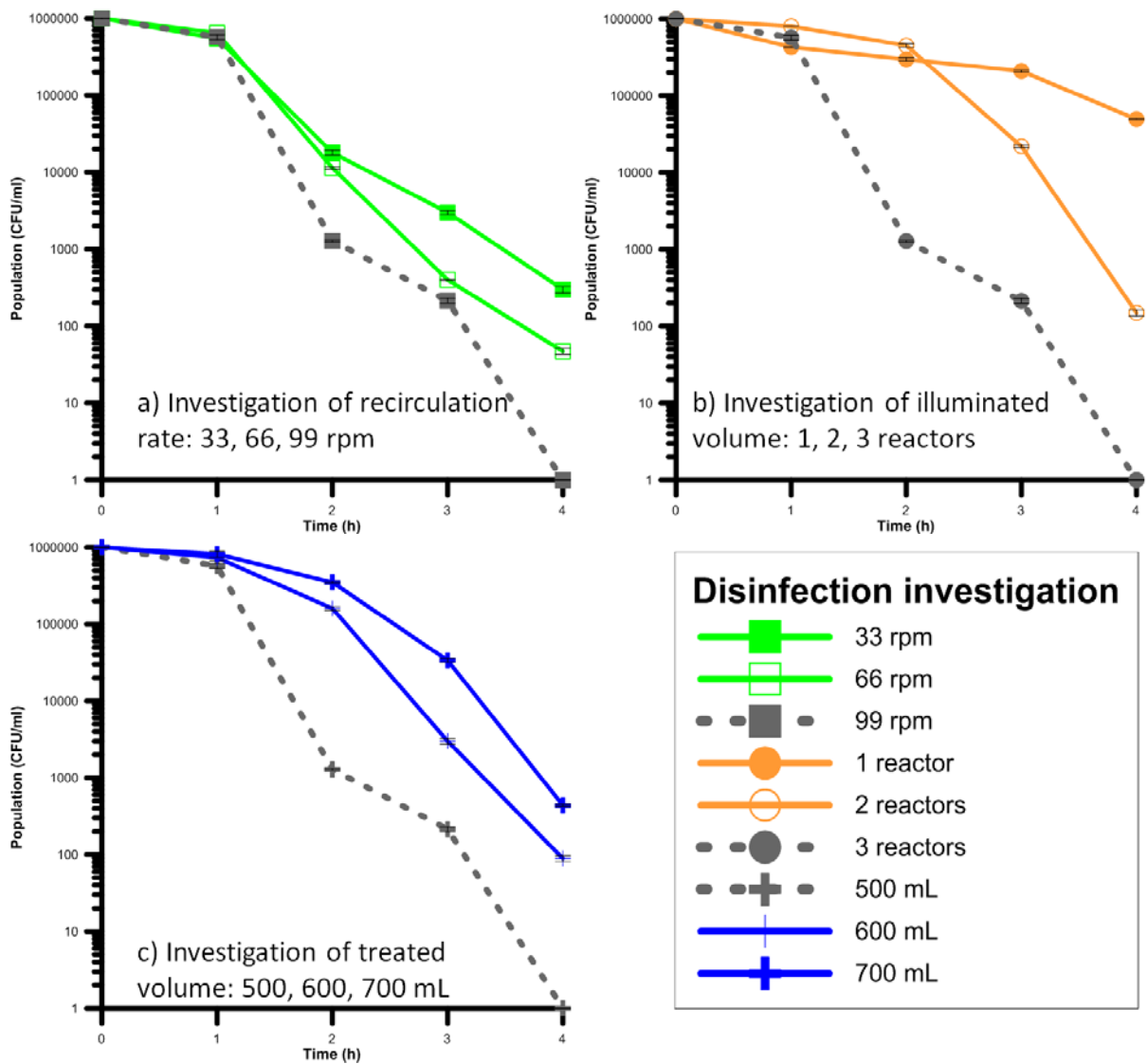
724

725

726

727

Figure 3 – Suggestion of the added actions sonication has towards bacterial inactivation, when coupled with photo-Fenton. The known photo-Fenton mechanisms suggested by literature are not displayed.



728

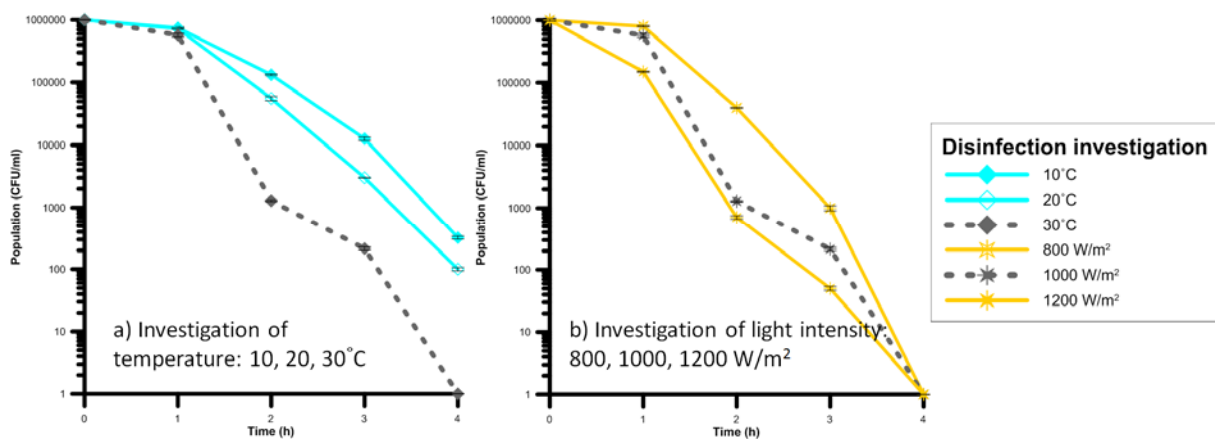
729

730

731

732

Figure 4 – Influence of the hydraulic characteristics of the experimental set-up, on the efficiency of the system. a) Investigation of the recirculation rate (33, 66 and 99 rpm), b) Investigation of the illuminated volume (1, 2 and 3 reactors) and c) Investigation on the effect of the treated volume (500, 600 and 700 mL).

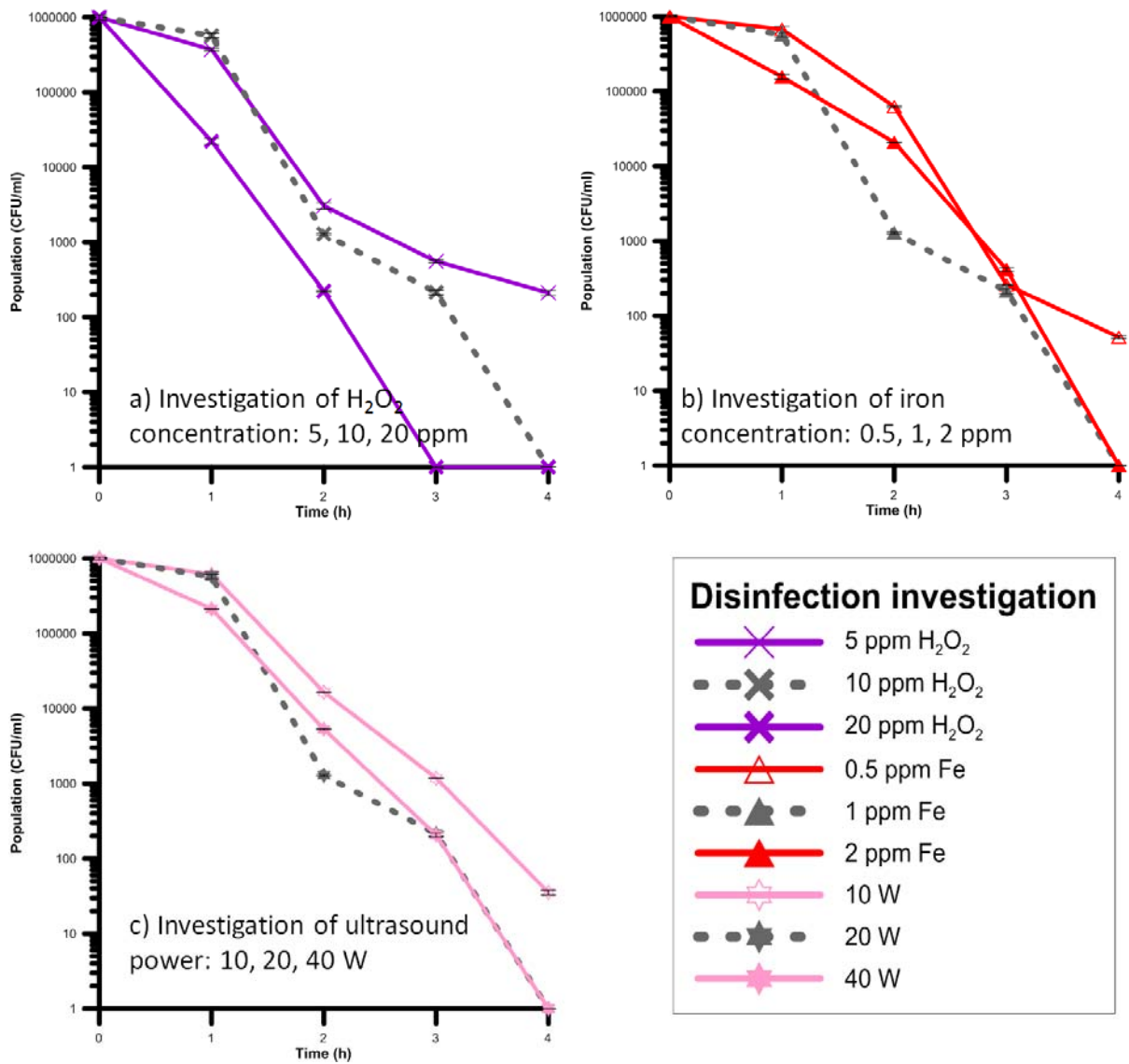


733

734

735

Figure 5 – Influence of the environmental parameters on the efficiency of the system. a) Investigation of temperature (10, 20 and 30°C), b) Investigation of light intensity (800, 1000 and 1200 W/m²).



736

737

738

739

Figure 6 - Influence of the Fenton reagents and the sonication intensity on the efficiency of the system. a) Investigation of the H₂O₂ concentration (5, 10 and 20 ppm), b) Investigation of the iron concentration (0.5, 1, and 2 ppm) and c) Investigation on the ultrasound power (10, 20 and 40 W).